JOURNAL OF MATERIALS SCIENCE 30 (1995) 5013–5019

Effect of the temperature dependence of thermal properties on the thermal shock tests of ceramics

T. NISHIKAWA, T. MIZUI, M. TAKATSU
Department of Materials Science and Engineering, Nagoya Institute of Technology, Gokiso-cho, Showa-ku, Nagoya 466, Japan
Y. MIZUTANI
Technical Research Institute, Toho Gas Co. Ltd, Shinpou-machi, Tokai-shi, Aichi 476, Japan

Thermal stress generated during a thermal shock is closely related to the fracture of ceramics. An attempt has been made to obtain thermal stress in a specimen by numerical calculation. The temperature dependence of thermal conductivity and diffusivity were introduced to realize the practical thermal conditions. The maximum thermal stress, σ^*_{max}, was recognized at the Fourier number, but differed from the temperature dependence. Correlative equations of σ^*_{max} and η^*_{max} with the Biot number, β_i, under cooling or heating tests, have been proposed. These equations resulted in the exact σ^*_{max} and η^*_{max} compared with the previous equations, in which temperature dependence was ignored. The thermal shock resistance parameter was expressed by the correlative equations of σ^*_{max} in order to suggest adequate experimental conditions and specimen size. A comparison of the measured and calculated time to failure of the specimen led to confirmation of the fracture criterion. The measured time disagreed with the calculated one, if the fracture by thermal shocking was not predominant. The correlative equations were also useful to select the kind of ceramics subjected to thermal shocking.

1. Introduction

Many methods have been proposed for the evaluation of thermal shock resistance of ceramics. The water-quenching method has been widely used in industry. In this method, the heated specimen is immersed in water and the residual strength is measured to define the critical temperature difference, $\Delta\theta_c$. On the other hand, for the rapid heating method, the decrease of strength is estimated by heating the specimen partially with infrared radiation, etc. However, the temperature dependence of thermal properties of ceramics has been ignored in these methods when calculating the thermal stress of the specimens.

In general, thermal conductivity and specific heat are significantly different for ceramics and change easily with temperature. These thermal properties greatly affect any evaluation by the thermal shock test. However, it is difficult to evaluate the thermal shock resistance of different ceramics with specimens of the same size because of the difference in their thermal properties. For example, a large specimen is needed for ceramics with large thermal conductivity. Secondly, ceramics subjected to a thermal shock are destroyed partially or entirely when maximum thermal stress is generated in them. However, the elastic strain energy remaining after the thermal shock test also affects the fracture of ceramics, prolonging the time to failure. Therefore, it is desirable to measure the time of fracture in thermal shock tests.

Many analyses of maximum thermal stress have been performed assuming constant thermal properties throughout the experiment. In the previous paper [1], the temperature dependence of thermal conductivity was found to contribute more to the maximum thermal stress during the thermal shock test. However, thermal diffusivity is also considered to affect the maximum thermal stress and Fourier number. This factor has not thus far been reported in the literature.

In the present work, thermal stress in an infinite plate was calculated numerically, by considering the temperature dependence of thermal conductivity and thermal diffusivity. Then, correlative equations of the maximum thermal stress and Fourier number were proposed as a non-linear function of the Biot number. A suitable size of specimens for the thermal shock test was suggested by using these equations. These numerical results are important as guidelines to estimate the exact thermal shock resistance and to select suitable ceramics for specific conditions.

2. Numerical method

Thermal stress and other parameters were easily obtained experimentally by the water-quench test,

0022–2461

supposing the heat conduction to be a one-dimensional problem [2]. Therefore, a numerical analysis was performed under the same condition for an actual thermal shock test, where thermal stress was generated in an infinite plate by the rapid heating or cooling of both surfaces. In this case, the following thermal conduction equation is given with the initial and boundary conditions

$$\partial/\partial\xi[\kappa^*(\partial T/\partial\xi)] = \partial T/\partial\eta_i \quad (1)$$

$$T = 0 \quad \text{at } \eta_i = 0 \quad (2)$$

$$\partial T/\partial\xi = 0 \quad \text{at } \xi = 0 \quad (3)$$

$$\pm\partial T/\partial\xi = \beta_i(T-1)/\lambda^* \quad \text{at } \xi = 1 \quad (4)$$

Non-dimensional thermal conductivity, λ^*, and thermal diffusivity, κ^*, in the above equations were expressed as a function of temperature, θ.

$$\lambda^* = \lambda/\lambda_i = 1 + AT \quad (5)$$

$$\kappa^* = \kappa/\kappa_i = 1 + BT \quad (6)$$

where T is the non-dimensional temperature shown as $(\theta-\theta_i)/(\theta_f-\theta_i)$ with temperature, θ. The non-dimensional length, ξ, is x/l, where x is the length from the centre and l is one-half the infinite plate thickness; η is the Fourier number shown as $\kappa t/l^2$ and β_i is the Biot number shown as hl/λ, where t is time and h is heat-transfer coefficient; κ is defined as $\lambda/\rho C_p$, where ρ is density and C_p is specific heat; and the subscripts i and f are the initial and final condition, respectively.

The coefficients A and B in Equations 5 and 6 are the coefficients of temperature dependence, denoted as temperature constants in this study. The non-dimensional thermal diffusivity, κ^*, was used instead of specific heat, C_p, for the following reasons. Thermal diffusivity is defined and expressed by thermal conductivity and specific heat. Thermal diffusivity is used in Equation 1 and numerical calculation becomes easy and simple using κ^*.

Equations 1–4 were rearranged to obtain the approximate thermal stress by the difference method, using the single-valued function of temperature F, $F = \int_0^T \kappa^* \, dT$ proposed by Goodman [3]. The following equations were thus obtained

$$\partial/\partial\xi[\kappa^*(\partial F/\partial\xi)] = \partial F/\partial\eta_i \quad (7)$$

$$F = 0 \quad \text{at } \eta_i = 0 \quad (8)$$

$$\partial F/\partial\xi = 0 \quad \text{at } \xi = 0 \quad (9)$$

$$\pm\partial F/\partial\xi = \beta_i F_f[\kappa^*/\lambda^*] \quad \text{at } \xi = 1 \quad (10)$$

Where $F_f = 1/B[1+(1+2BF)^{1/2}] - 1$. The details are given in the Appendix. The partial differential equation of Equation 7 was solved numerically by the Crank–Nicolson (implicit) method [4]. In this calculation process, the approximate difference equation of time and that of conditions were applied to the left side and right side of each equation, respectively. Compared with the previous (explicit) method [1], high secondary accuracy of time, stable calculation and a relatively small amount of calculation were the advantages of this method.

The temperature distribution of the specimen with time was calculated under constant β_i and temperature coefficients A and B. The mean temperature along the thickness of the infinite plate, T_{mean}, was given by

$$T_{mean} = \int_0^T T(\xi)\,d\xi \quad (11)$$

Thermal stress under a given Fourier number, η, can be calculated as follows [5]

$$\sigma^*(\xi) = T_{mean} - T(\xi) \quad (12)$$

where σ^* is the non-dimensional thermal stress shown as $\sigma_f/[\alpha E\Delta\theta]$, σ_f is fracture strength, α is thermal expansion coefficient, E is Young's modulus, and $\Delta\theta$, the absolute value of $\theta_f - \theta_i$, is the temperature difference in the thermal shock test. The maximum tensile stress is generated at $\xi = 0$ (surface of the specimen) for rapid heating and at $\xi = 1$ (centre of specimen) for rapid cooling, respectively. The curve of σ^* with η has a maximum, so the maximum thermal stress σ^*_{max} is judged from the positive or negative $(\sigma^*_n - \sigma^*_{n-1})$ value. The subscript n indicates the nth value divided by the Fourier number, η. Fourier number at maximum thermal stress is expressed as η^*_{max}.

3. Correlative equations

3.1. Correlative equation of maximum thermal stress, σ^*_{max}

Maximum thermal stress, σ^*_{max}, was calculated by the above method, where the temperature coefficients of thermal conductivity and thermal diffusivity were used. From the numerical results, the relation between $1/\sigma^*_{max}$ and $1/\beta_i$ was not expressed as the following linear function [6]

$$1/\sigma^*_{max} = a + b/\beta_i \quad (13)$$

Therefore, a corrective term was introduced on the right-hand side of the equation

$$1/\sigma^*_{max} = a_s + b_s/\beta_i + (1-a_s)\exp(c_s/\beta_i + d_s) \quad (14)$$

on rapid cooling

$$1/\sigma^*_{max} = e_s + f_s/\beta_i + g_s\exp(-2/\beta_i) \quad (15)$$

on rapid heating.

Parameters a_s–g_s were obtained by the least squares method. The subscript s in Equations 14 and 15 refers to the parameters related to the determination of σ^*_{max}. The two equations were proposed due to the different convex and concave curve, where a monotonic increase was observed. On rapid cooling, parameters a_s and b_s depended on the temperature coefficients A and B; c_s and d_s depended only on A. On rapid heating, all parameters e_s, f_s and g_s depended on the temperature coefficients A and B. The numerical results of the correlative equation of σ^*_{max} are given in

TABLE I Correlative equations and parameters of maximum thermal stress

Correlative equation on rapid cooling

$1/\sigma^*_{max} = a_s + b_s/\beta_i + (1 - a_s)\exp(c_s/\beta_i + d_s)$

$a_s = X_1 + X_2\exp(X_3 B)$

$X_1 = 0.734 + 0.675\,(A+1)^{0.570}$

$X_2 = -0.135 + 0.247\,(A+1)^{0.441}$

$X_3 = -0.378 - 0.949\,(A+1)^{-0.638}$

$b_s = Y_1 + Y_2 B + Y_3 B^2$

$Y_1 = 2.181 + 1.099\,(A+1)^{0.510}$

$Y_2 = -1.902 + 1.692\,(A+1)^{0.049}$

$Y_3 = -0.539 + 0.556\,(A+1)^{-0.024}$

$c_s = -6.163 - 2.213\,(A+1)^{-1.454}$

$d_s = -0.179 - 0.144\,(A+1)^{-0.749}$

Correlation equation on rapid heating

$1/\sigma^*_{max} = e_s + f_s/\beta_i + g_s\exp(-2/\beta_i)$

$e_s = X_1 + X_2\exp(X_2 B)$

$X_1 = -2.198 + 3.562\,(A+1)^{0.379}$

$X_2 = -0.539 + 2.678\,(A+1)^{0.500}$

$X_3 = 0.039 - 0.925\,(A+1)^{-0.491}$

$f_s = -B + Y_1 + Y_2\,(B+1)^{-0.4}$

$Y_1 = 0.550 + 2.780\,(A+1)^{-0.343}$

$Y_2 = 9.620 - 6.639\,(A+1)^{-0.134}$

$g_s = Z_1 + Z_2\exp(Z_3 B)$

$Z_1 = -4.214 + 5.264\,(A+1)^{-0.248}$

$Z_2 = -0.777 - 1.222\,(A+1)^{0.965}$

$Z_3 = -0.006 - 0.846\,(A+1)^{-0.852}$

TABLE II Correlative equations and parameters of Fourier number at maximum thermal stress

Correlative equation on rapid cooling

$\eta^*_{max} = a_t + b_t\beta_i^{ct}$

$a_t = X_1 A + X_2(A+1)^{1.2}$

$X_1 = -0.003 + 0.018\,(B+1)^{-0.776}$

$X_2 = 0.029 - 0.053\,(B+1)^{-0.308}$

$b_t = Y_1 + Y_2 A + Y_3(A+1)^{0.5}$

$Y_1 = 0.819 - 0.451\,(B+1)^{0.263}$

$Y_2 = 0.385 - 0.330\,(B+1)^{0.085}$

$Y_3 = -0.542 + 0.391\,(B+1)^{0.185}$

$c_t = Z_1 + Z_2\ln(A+1)$

$Z_1 = 0.336 - 0.844\,(B+1)^{0.200}$

$Z_2 = 0.235 - 0.030\,(B+1)^{-0.123}$

Correlative equation on rapid heating

$1/\eta^*_{max} = d_t + e_t\exp(f_t/\beta_i)$

$d_t = X_1 - 0.65\exp(X_2 A)$

$X_1 = 3.723 + 0.620\,(B+1)^{0.958}$

$X_2 = -0.954 - 0.191\,(B+1)^{1.236}$

$e_t = Y_1 + Y_2\exp(-0.8A)$

$Y_1 = 0.913 + 2.399\,(B+1)^{0.962}$

$Y_2 = 0.696 + 0.808\,(B+1)^{0.519}$

$f_t = Z_1 - 5(A+1)^{Z2}$

$Z_1 = 3.723 + 0.620\,(B+1)^{0.958}$

$Z_2 = -0.954 - 0.191\,(B+1)^{1.237}$

Table I. If the temperature dependence is ignored, that is $A = B = 0$, the parameter $a_s = 1.51$ and $b_s = 3.29$ at rapid cooling, while $e_s = 3.49$ and $f_s = 6.33$ at rapid heating. These values agreed with the previous correlative equation [1].

3.2. Correlative equation of the Fourier number, η^*_{max}, at σ^*_{max}

Measured time to failure on the thermal shock test must agree with that calculated at maximum thermal stress, if the specimen is destroyed only by the generated thermal stress. Rogers *et al.* [7] obtained experimentally the distribution of failure probability as a function of time to failure. In this study, the following correlative equations of Fourier number, η^*_{max}, were used

$$\eta^*_{max} = a_t + b_t\beta_i^{Ct} \tag{16}$$

on rapid cooling

$$1/\eta^*_{max} = d_t + e_t\exp(f_t/\beta_i) \tag{17}$$

on rapid heating.

Parameters a_t–f_t were obtained by the method of least squares. The subscript t in Equations 16 and 17 refers to the parameters for determination of η^*_{max}. All parameters were dependent on the temperature coefficients A and B. The numerical correlative equations of Fourier number, η^*_{max}, at σ^*_{max} are listed in Table II.

4. Discussion

4.1. Accuracy of temperature constants A and B

Satymurthy *et al.* [8] used the following approximate equation to express the thermal conductivity as a function of temperature

$$\lambda = \lambda_0/\theta + \lambda_1 \tag{18}$$

where λ_0 and λ_1 were constants. However, this equation was only applied to a rapid heating test, where the thermal conductivity decreased with temperature increase. It is not reasonable that λ^* becomes infinite at $T = 0$ in the non-dimensional form. In the present study, thermal conductivity and thermal diffusivity were defined by Equations 5 and 6, where these values could be expressed as a linear function of temperature within the experimental range. These expressions were earlier used by Koizumi and Taniwaki [9] to obtain the thermal stress of the cylindrical specimen in the cooling test.

To determine the temperature coefficients from the thermal properties, the measured thermal conductivity and diffusivity were normalized as the non-dimensional $\lambda^* = \lambda/\lambda_i$, $\kappa^* = \kappa/\kappa_i$. These values were plotted with the non-dimensional temperature, T, to approximate with Equation 5 and 6. The slope of the straight line showed the temperature coefficient A or B. Thus, the temperature coefficients A and B often change with the temperature difference, $\Delta\theta_{obs}$, in the thermal shock test. The subscript obs indicates the experimental value. Alumina showed small $\Delta\theta_{obs}$, and the linear temperature dependence caused the constant values of A and B. However, the difference between measured and calculated values from Equation 5 or 6 cannot be ignored for ceramics having a scattered $\Delta\theta_{obs}$ in thermal shock test. For example, silicon nitride showed the large critical temperature difference, $\Delta\theta_c$, and a non-linear temperature dependence. It is not reasonable to give a temperature coefficient throughout the experiment.

In practice, it is desirable to carry out the numerical calculation at $\Delta\theta_{obs}$ near the $\Delta\theta_c$ measured previously by other methods. In the case of scattered $\Delta\theta_{obs}$, the use of a large specimen or a curve approximation of the temperature dependence is recommended. The

preparation of a large specimen makes it easier to perform the test, so the specimen should be large to reduce the difference between coefficients A and B.

4.2. Effect of temperature coefficients A and B on thermal stress

4.2.1. Rapid cooling condition

The changes of thermal stress on the specimen surface with time are shown in Fig. 1 for rapid cooling. The curves had different temperature coefficients A and B. The maximum in each curve corresponded to the maximum thermal stress, σ^*_{max}, and Fourier number, η^*_{max}. Curve I_q indicates the thermal stress of ceramics having a significant temperature dependence of thermal conductivity and thermal diffusivity ($A = 3$, $B = 5$ as typical examples). Curve II_q indicates thermal stress of ceramics having only temperature dependence of thermal diffusivity ($A = 0$, $B = 5$). The temperature dependence of thermal properties was not considered for curve III_q, that is $A = B = 0$. The subscript q refers to the rapid cooling condition.

Comparing the three curves, we note that the σ^*_{max} of curve I_q was smaller than that of curve III_q. The temperature gradient near the surface becomes less sharp because of the introduction of large non-dimensional thermal conductivity as the denominator to the equation of the boundary condition, Equation 4. Consequently, the specimen was entirely cooled in a short time. For ceramics having only the temperature dependence of thermal diffusivity, the σ^*_{max} of curve II_q was larger than that for curve III_q. As the change in temperature near the surface is enhanced, the temperature difference between the surface and inside increases, resulting in a large thermal stress in the specimen.

The temperature distribution of the specimen is shown in Fig. 2, when the maximum thermal stress for curves I_q and II_q is generated. Average temperatures, T_m, at maximum thermal stress and σ^*_{max} are also shown schematically. The values of η^*_{max} were 0.037 at curve I_q and 0.023 at curve II_q, respectively. The small temperature gradient near the surface is shown for the ceramics having both temperature dependences, that is for curve I_q, while a sharp temperature gradient is shown for the ceramics having thermal conductivity independent of temperature. The average temperature of the specimen, T_m, was hardly affected by the temperature dependence. The difference between surface temperature and T_m corresponded to σ^*_{max} at rapid cooling. Therefore, large σ^*_{max} was observed for the ceramics having the thermal conductivity independent of temperature.

The Fourier number η^*_{max} at maximum thermal stress changed with the sign of temperature coefficients A and B. When the coefficients are positive (i.e. increasing thermal conductivity and diffusivity with decreasing temperature), η^*_{max} shifted towards the short-time side. The large temperature difference in the specimen was generated and observed for a short time. When the coefficients are negative, η^*_{max} shifted towards the opposite, long-time side. The σ^*_{max} and η^*_{max} in the specimen were affected by the temperature

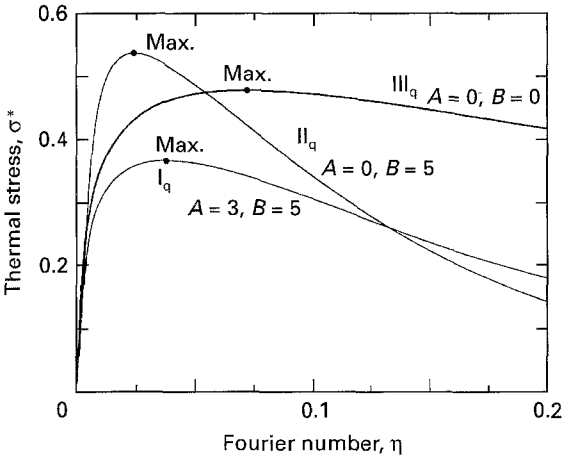

Figure 1 Changes of thermal stress on the specimen surface with Fourier number under rapid cooling. Specimens had different temperature coefficients A and B, but constant Biot number $\beta_i = 5$.

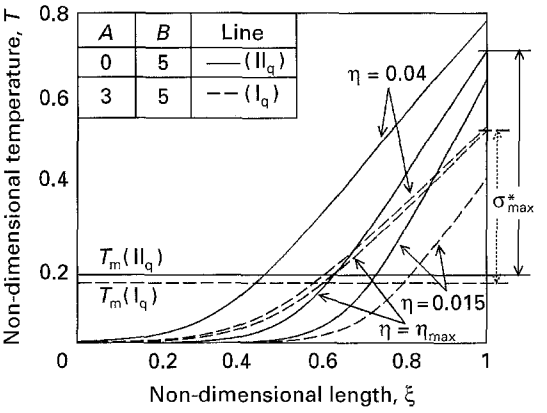

Figure 2 Temperature distribution of the specimen under rapid cooling near the maximum thermal stress. Temperature coefficients agree with those in Fig. 1.

dependence of the thermal conductivity and diffusivity, but the former dependence was more predominant than the latter.

4.2.2. Rapid heating condition

The changes of thermal stress at the specimen centre with time are shown in Fig. 3 under rapid heating. The maximum in each curve corresponded to σ^*_{max}. The curves had different temperature constants A and B, which corresponded to those under rapid cooling, but the sign became the opposite. The essential temperature dependence of thermal properties in curves I_h, II_h and III_h agreed with that in Fig. 1, respectively. The subscript h indicates the rapid heating condition.

The σ^*_{max} of curve I_h was larger, and that of curve II_h was smaller, than that of curve III_h. However, the difference between these values and the effects of temperature dependence of thermal properties were small compared with those at rapid cooling. Temperature distributions in the specimen at the maximum thermal stress for curves I_h and II_h, are shown in Fig. 4. The σ^*_{max} at rapid heating decreased approximately by one-half compared with that at rapid cooling. The fracture origin is the centre of the specimen on heating,

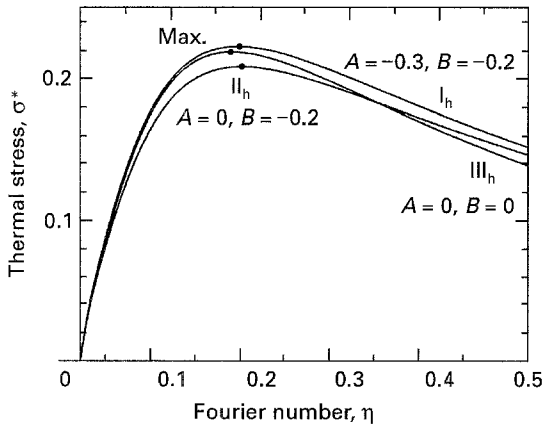

Figure 3 Changes of thermal stress on the specimen surface with Fourier number under rapid heating. Specimens had different temperature coefficients A and B, but constant Biot number $\beta_i = 5$.

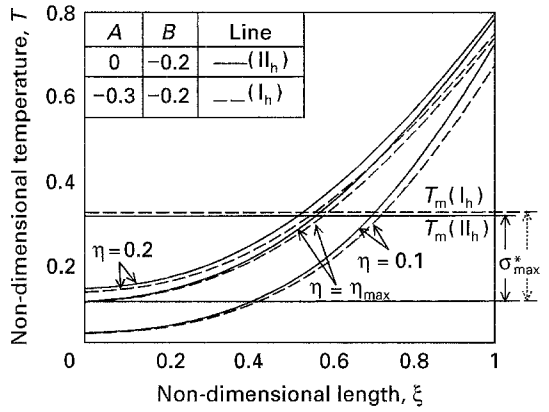

Figure 4 Temperature distribution of the specimen under rapid heating near the maximum thermal stress. Temperature coefficients agree with those in Fig. 3.

but on the surface on cooling. Therefore, the difference between the centre temperature and the average temperature becomes small on rapid heating, resulting in small σ^*_{max}. The η^*_{max} on heating elongated significantly compared with that on cooling. The slow change in temperature in the centre caused this large η^*_{max}.

The effect of the temperature dependence of thermal conductivity and diffusivity on the thermal shock test was different between the heating and cooling tests. Maximum thermal stress decreased on cooling, but increased on heating for the ceramics having the temperature dependence of thermal conductivity. The thermal shock resistance parameter on cooling or heating cannot be compared without considering the temperature dependence of thermal properties.

4.3. Applied conditions of the correlative equation

The adequate temperature coefficients, A, B, and Biot number, β_i, must be estimated to utilize the correlative equation of σ^*_{max} and η^*_{max} in the applied temperature region. On calculation, the recommended correlative equations can be used for the materials having A and B values ranging from -1 to 5. The applied conditions for ceramics are detailed below.

The temperature dependence of thermal conductivity, A, is relatively constant because of the small temperature difference in the rapid cooling test. Where the thermal diffusivity is defined to be $\kappa = \lambda/\rho C_p$, the temperature dependence of thermal diffusivity, B, contributes to those of thermal conductivity and specific heat. Most ceramics are considered to have A and B values ranging from 0–5.

The initial temperature, θ_i, indicates the heating temperature on cooling and the room temperature on heating tests, respectively. Therefore, the temperature coefficients A and B on heating have the opposite sign and reciprocal number of those on cooling. The range of coefficients A and B during the heating test was considered to be from -1 to 0 for most ceramics.

The range of Biot number, β_i, was considered to be $1 \leqslant \beta_i \leqslant 50$ for both thermal shock tests. This number changes due to the thermal conduction condition between the specimen surface and the surrounding medium (i.e. water, oil or air). However, because β_i can be controlled by changing the specimen size, l, the above range was considered to be reasonable in practice. A large specimen was often necessary for the thermal shock test.

4.4. Critical temperature difference, $\Delta\theta_c$

The thermal shock resistance of ceramics was frequently evaluated by the water quenching method in the literature, where $\Delta\theta_c$ was obtained from the drastic decrease of strength at a given temperature difference. Substituting the correlative equation of σ^*_{max} into $\sigma^*_{max} = \sigma_f/\alpha E\Delta\theta_c = R/\Delta\theta_c$, where R is thermal shock resistance parameter, θ_c is given by

$$\Delta\theta_c = R[a_s + b_s/\beta_i + (1 - a_s)\exp(c_s/\beta_i + d_s)] \quad (19)$$

on rapid cooling

$$\Delta\theta_c = R[e_s + f_s/\beta_i + g_s\exp(-2/\beta_i)] \quad (20)$$

on rapid heating

The parameters a_s–g_s are listed in Table I. The relation between $\Delta\theta_c$ and β_i for the ceramics having a temperature dependence of thermal properties is shown in Fig. 5. The curves were obtained from the curve I_q in Fig. 1 and curve I_h in Fig. 3, where the essential temperature dependences were the same. The dotted lines in the figure indicate the fracture limit under which ceramics were not fractured by a thermal shock. A significantly different $\Delta\theta_c$ was observed in the cooling or heating test. A different σ_{max} was generated with a different fracture origin. A rapid change of temperature on the surface generated large thermal stress on cooling, whereas a slow change in the centre caused low thermal stress on heating.

For ceramics having a temperature dependence of thermal properties, a sharp change of $\Delta\theta_c$ was observed with β_i. A remarkably different $\Delta\theta_c$ was obtained even with a small change in test conditions. Therefore, several $\Delta\theta_c$ values must be measured by changing β_i, using several specimen sizes or different surrounding conditions. In practice, it was most

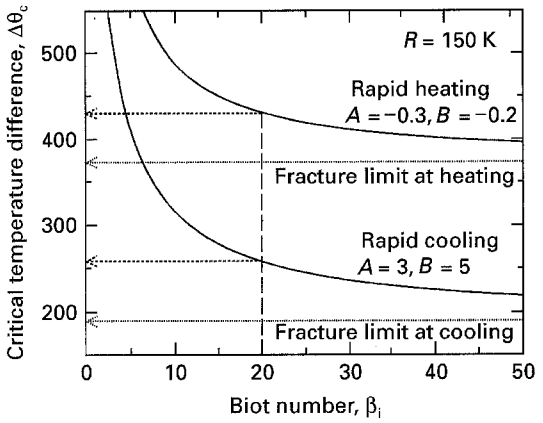

Figure 5 Changes of critical temperature difference with Biot number and each fracture limit. Curves show the rapid heating and cooling of the same ceramics.

convenient to change the specimen size. A thermal shock test must be performed with several specimen sizes to obtain the exact constant R. The difference between $\Delta\theta_c$ obtained by cooling and heating changes not only with thermal conductivity and diffusivity, but also with the temperature dependence. Adequate ceramics must be selected for industrial thermal conditions on the basis of the above heat parameters.

4.5. Confirmation of the thermal shock test

The $\Delta\theta_c$ and σ^*_{max} are constants at a given condition and can be obtained by the thermal shock test. However, the contribution of the elastic strain energy to fracture must be noted. The fracture occurred either by thermal stress or elastic strain energy. This fracture criterion must be determined by measuring time to failure. If the measured time to failure agrees with that calculated from the correlative equation of η^*_{max}, only thermal stress contributes to the fracture of the ceramics. The fracture caused in connection with strain energy prolongs the time to failure. Therefore, these thermal shock test data must be excluded from the calculation. It is also important to obtain the exact time to failure in the experiment.

5. Conclusions

The thermal stress and Fourier number were obtained from the numerical calculation, supposing the heat conduction to be a one-dimensional problem. Non-dimensional thermal conductivity and diffusivity were used as a function of temperature in the calculation. The following conclusions were obtained.

1. Correlative equations of maximum thermal stress, σ^*_{max}, and Fourier number, η^*_{max}, were proposed using temperature correlations of thermal properties.
2. For the rapid cooling test, σ^*_{max} and η^*_{max} were affected by the temperature dependence of thermal conductivity and diffusivity. The former dependence was more predominant than the latter.
3. The σ^*_{max} at rapid heating decreased approximately by one-half, independently of temperature correlations, compared with that at rapid cooling.
4. For ceramics having a temperature dependence of thermal properties, a sharp change of critical temperature difference, $\Delta\theta_c$, was observed with Biot number, β_i. A remarkably different $\Delta\theta_c$ was obtained even with a small change in test conditions. Therefore, several $\Delta\theta_c$ values must be measured by changing β_i to evaluate the thermal shock resistance.
5. The fracture criterion can be assumed by comparison of measured and calculated time to fracture. If the measured time agrees with that calculated from the correlative equations, only thermal stress contributes to the fracture of the ceramics.

Appendix. Thermal conduction equation on rapid cooling or heating of an infinite plate

The heat conduction equation for an infinite plate, which was heated or cooled uniformly on both surfaces, is given with initial and boundary conditions by

$$\partial/\partial\xi[\kappa^*(\partial T/\partial\xi)] = \partial T/\partial\eta_i \quad \text{(A1)}$$

$$T = 0 \quad \text{at } \eta_i = 0 \quad \text{(A2)}$$

$$\partial T/\partial\xi = 0 \quad \text{at } \xi = 0 \quad \text{(A3)}$$

$$\pm\partial T/\partial\xi = \beta_i(T - 1)/\lambda^* \quad \text{at } \xi = 1 \quad \text{(A4)}$$

Non-dimensional thermal conductivity, λ^*, and thermal diffusivity, κ^*, in the above equations were expressed as a function of temperature, θ

$$\lambda^* = \lambda/\lambda_i = 1 + AT \quad \text{(A5)}$$

$$\kappa^* = \kappa/\kappa_i = 1 + BT \quad \text{(A6)}$$

where T is non-dimensional temperature shown as $(\theta - \theta_i)/(\theta_f - \theta_i)$ with temperature, θ.

Equations A 1–4 were rearranged by the difference method, using a single-valued function of temperature, F, which was expressed below according to Goodman

$$F = \int_0^T \kappa^* \, dT \quad \text{(A7)}$$

Equation A1 can be arranged, using $\partial F = \kappa^* \partial T$ to give

$$\partial/\partial\xi[\partial F/\partial\xi] = (1/\kappa^*)[\partial F/\partial\eta_i]$$

$$\therefore \partial/\partial\xi[\kappa^*(\partial F/\partial\xi)] = \partial F/\partial\eta_i \quad \text{(A8)}$$

Substituting Equation A6 into Equation A7, we have

$$F = T + (1/2)BT^2 \quad \text{(A9a)}$$

or

$$T = (1/B)[1 \pm (1 + 2BF)^{1/2}] \quad \text{(A9b)}$$

Because T is always positive, the above equation is also given by

$$T = (1/B)[1 + (1 + 2BF)^{1/2}] \quad \text{(A10)}$$

Substituting Equation A2 into Equation A9a gives

$$F = 0 \quad \text{at } \eta_i = 0 \tag{A11}$$

Using $(1/\kappa^*)[\partial F/\partial \xi] = 0$ from Equation A3 and $\partial F = \kappa^* \partial T$ from Equation A7 yields

$$\partial F/\partial \xi = 0 \quad \text{at } \xi = 0 \tag{A12}$$

The following equation was then obtained from Equation A4, using factor F

$$\pm \partial F/\partial \xi = \beta_i (T - 1)\kappa^*/\lambda^* \tag{A13}$$

The following equation is introduced into the above equation

$$F_f = T - 1 = (1/B)[1 + (1 + 2BF)^{1/2}] - 1 \tag{A14}$$

The boundary condition may be stated

$$\pm \partial F/\partial \xi = \beta_i F_f [\kappa^*/\lambda^*] \quad \text{at } \xi = 1 \tag{A15}$$

Therefore, the rearranged heat equation and conditions are as follows

$$\partial/\partial \xi [\kappa^* (\partial F/\partial \xi)] = \partial F/\partial \eta_i \tag{A16}$$

$$F = 0 \quad \text{at } \eta_i = 0 \tag{A17}$$

$$\partial F/\partial \xi = 0 \quad \text{at } \xi = 0 \tag{A18}$$

$$\pm \partial F/\partial \xi = \beta_i F_f [\kappa^*/\lambda^*] \quad \text{at } \xi = 1 \tag{A19}$$

in which $F_f = 1/B[1 + (1 + 2BF)^{1/2}] - 1$.

References

1. M. TAKATSU, T. NISHIKAWA and Y. MIZUTANI, *Kagaku Kougaku Ronbunshu* **19** (1993) 633.
2. T. NISHIKAWA, T. GAO, M. HIBI, M. TAKATSU and M. OGAWA, *J. Mater. Sci.* **29** (1994) 213.
3. T. R. GOODMAN, *J. Heat Transfer* **83** (1961) 83.
4. Y. OHNO and K. ISODA, "Suuchi keisan handbook" (Ohm Sha, Tokyo, 1988) p. 119.
5. S. P. TIMOSHENKO and J. N. GOODIER, "Theory of elasticity" (McGraw-Hill, New York, 1970)
6. S. S. MANSON and R. W. SMITH, *Trans. ASME* **78** (1956) 533.
7. W. P. ROGERS, A. F. EMERY, R. C. BRADT and A. S. KOBAYASHI, *J. Am. Ceram. Soc.* **70** (1987) 406.
8. K. SATYMURTHY, J. P. SINGH, D. P. H. HASSELMAN and M. P. KAMAT, *ibid.* **63** (1980) 363.
9. T. KOIZUMI and C. TANIWAKI, *Trans. JSME* **A31** (1965) 221.

Received 2 March 1994
and accepted 28 April 1995